

Some useful references, taken from the bibliography:

Tests of three-flavor mixing in long-baseline neutrino oscillation experiments

G. L. Fogli

Dipartimento di Fisica dell'Università and Sezione INFN di Bari, I-70126 Bari, Italy

E. Lisi

Institute for Advanced Study, Princeton, New Jersey 08540, U.S.A.

and Dipartimento di Fisica dell'Università and Sezione INFN di Bari, I-70126 Bari, Italy

We compare the effectiveness of various tests of three-flavor mixing in future long-baseline neutrino oscillation experiments. We analyze a representative case of mixing in a simplified three-flavor scheme, whose relevant parameters are one neutrino mass-square difference, m^2 , and two mixing angles, ψ and ϕ . We show that an unambiguous determination of ψ and ϕ requires flavor-appearance tests in accelerator experiments, as well as supplementary information from reactor experiments.

PACS number(s): 14.60.Pq, 12.15.Ff, 14.60.Lm

[hep-ph/9604415]

If θ_{13} is 0,
there is no CP
violation!

Prospects of accelerator and reactor neutrino oscillation experiments for the coming ten years

[hep-ph/0403068]

P. HUBER^a, M. LINDNER^b, M. ROLINEC^c,
T. SCHWETZ^d, AND W. WINTER^e

Abstract

We analyze the physics potential of long baseline neutrino oscillation experiments planned for the coming ten years, where the main focus is the sensitivity limit to the small mixing angle θ_{13} . The discussed experiments include the conventional beam experiments MINOS, ICARUS, and OPERA, which are under construction, the planned superbeam experiments J-PARC to Super-Kamiokande and NuMI off-axis, as well as new reactor experiments with near and far detectors, represented by the Double-Chooz project. We perform a complete numerical simulation including systematics, correlations, and degeneracies on an equal footing for all experiments using the GLoBES software. After discussing the improvement of our knowledge on the atmospheric parameters θ_{23} and Δm_{31}^2 by these experiments, we investigate the potential to determine θ_{13} within the next ten years in detail. Furthermore, we show that under optimistic assumptions and for θ_{13} close to the current bound, even the next generation of experiments might provide some information on the Dirac CP phase and the type of the neutrino mass hierarchy.

$$\begin{aligned}
P(\nu_\mu \rightarrow \nu_e) &\simeq \sin^2 2\theta_{13} \sin^2 \theta_{23} \sin^2 \Delta \\
&\mp \alpha \sin 2\theta_{13} \sin \delta_{\text{CP}} \sin 2\theta_{12} \sin 2\theta_{23} \Delta \sin^2 \Delta \\
&+ \alpha \sin 2\theta_{13} \cos \delta_{\text{CP}} \sin 2\theta_{12} \sin 2\theta_{23} \Delta \cos \Delta \sin \Delta \\
&+ \alpha^2 \cos^2 \theta_{23} \sin^2 2\theta_{12} \Delta^2
\end{aligned}
\quad \Delta \equiv \Delta m_{31}^2 L / (4E_\nu).$$

Huber, *etal.*

$$1 - P_{\bar{e}\bar{e}} \simeq \sin^2 2\theta_{13} \sin^2 \Delta + \alpha^2 \Delta^2 \cos^4 \theta_{13} \sin^2 2\theta_{12}. \quad (2)$$

of $\sin^2 2\theta_{13}$ [20]. These parameters can be only measured by the $\nu_\mu \rightarrow \nu_\mu$, $\nu_\mu \rightarrow \nu_e$, and $\nu_\mu \rightarrow \nu_\tau$ channels in beam experiments. However, comparing Eqs. (1) and (2), one can easily see that reactor experiments should allow a “clean” and degenerate-free measurement of $\sin^2 2\theta_{13}$ [19]. In contrast, the determination of $\sin^2 2\theta_{13}$ using the appearance channel in Eq. (1) is strongly affected by the more complicated parameter dependence of the oscillation probability, which leads to multi-parameter correlations [27] and to the (δ, θ_{13}) [37], $\text{sgn}(\Delta m_{31}^2)$ [38], and $(\theta_{23}, \pi/2 - \theta_{23})$ [39] degeneracies, *i.e.*, an overall “eight-fold” degeneracy [40]. In the analysis, we take into account all of these degeneracies. Note however, that the $(\theta_{23}, \pi/2 - \theta_{23})$ degeneracy is not present, since we always adopt for the true value of θ_{23} the current atmospheric best-fit value $\theta_{23} = \pi/4$. The proper treatment of correlations and

$$\begin{aligned}
\sin^2(2\theta_{12}) &= 0.8_{-0.1}^{+0.15} & \sin^2(2\theta_{23}) &= 1_{-0.15}^{+0} & |\Delta m_{31}^2| &= 2.0_{-0.9}^{+1.2} \cdot 10^{-3} \text{ eV}^2, \\
\theta_{12} &\sim 32^0 & \theta_{23} &\sim 39^0 & \Delta m_{21}^2 &= 7.0_{-1.6}^{+2.5} \cdot 10^{-5} \text{ eV}^2, \\
28^0 &< \theta_{12} < 39^0 & 33^0 &< \theta_{23} < 45^0 & \sin^2 2\theta_{13} &\leq 0.14 (0.25), \\
0.23 &< \sin^2(\theta_{12}) < 0.39 & 0.3 &< \sin^2(\theta_{23}) < 0.5 & &
\end{aligned}$$

$$U = \begin{bmatrix} c_{12}c_{13} & s_{12}c_{13} & s_{13}e^{-i\delta} \\ -s_{12}c_{23} - c_{12}s_{23}s_{13}e^{i\delta} & c_{12}c_{23} - s_{12}s_{23}s_{13}e^{i\delta} & s_{23}c_{13} \\ s_{12}s_{23} - c_{12}c_{23}s_{13}e^{i\delta} & -c_{12}s_{23} - s_{12}c_{23}s_{13}e^{i\delta} & c_{23}c_{13} \end{bmatrix}$$

Use average values
from current measurements

U is identically unitary. Plugging in known
values of θ_{12} and θ_{23} does not constrain θ_{13} .

s12	0.525731 ~32 deg		0.850651 c13		0.525731 c13		s13
c12	0.850651						
		-0.40815	-0.53616 s13	0.660406	-0.33137 s13	0.630298 c13	
s23	0.630298 ~39 deg						
c23	0.776353	0.331367	-0.66041 s13	-0.53616	-0.40815 s13	0.776353 c13	

	0.723607	c13^2		0.276393	c13^2	s13^2	=1
0.166589	0.437674 s13	0.287471 s13^2	0.436136	-0.43767 s13	0.109804 s13^2	0.397276 c13^2	=1
0.109804	-0.43767 s13	0.436136 s13^2	0.287471	0.437674 s13	0.166589 s13^2	0.602724 c13^2	=1

	0.723607 c13^2	0.276393 c13^2	s13^2	=1
0.602724	0 s13	0.397276 s13^2	0.397276 c13^2	=1
0.397276	0 s13	0.602724 s13^2	0.602724 c13^2	=1

Disappearance and appearance experiments
measure different quantities:

**Super-K / Minos /
T2K Measures** $\longrightarrow P(\nu_\mu \rightarrow \nu_x) = \boxed{\sin^2 2\theta_{23}} \sin^2 \left(\frac{1.27 \Delta m_{23}^2 L}{E_\nu} \right)$

Offaxis θ_{13} Measures $\longrightarrow P(\nu_\mu \rightarrow \nu_e) = \boxed{\sin^2 \theta_{23}} \sin^2 2\theta_{13} \sin^2 \left(\frac{1.27 \Delta m_{13}^2 L}{E_\nu} \right)$

Measurement with $\sin^2 2\theta_{23} = 0.95 \pm 0.01$

$$\Rightarrow \theta_{23} = 38^\circ \text{ or } 52^\circ$$

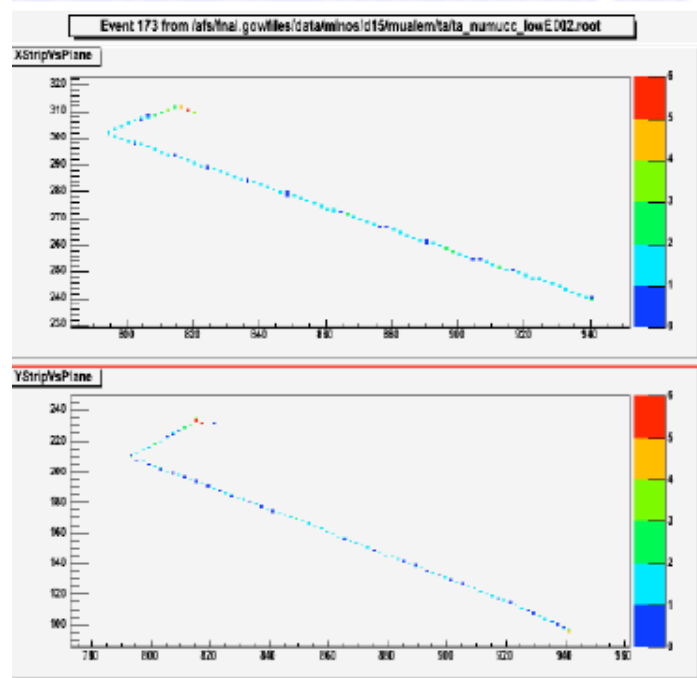
Prediction for appearance rate $\propto \sin^2 \theta_{23}$

$$\Rightarrow \sin^2 \theta_{23} = 0.38 \text{ or } 0.62$$

(x1.6 uncertainty)



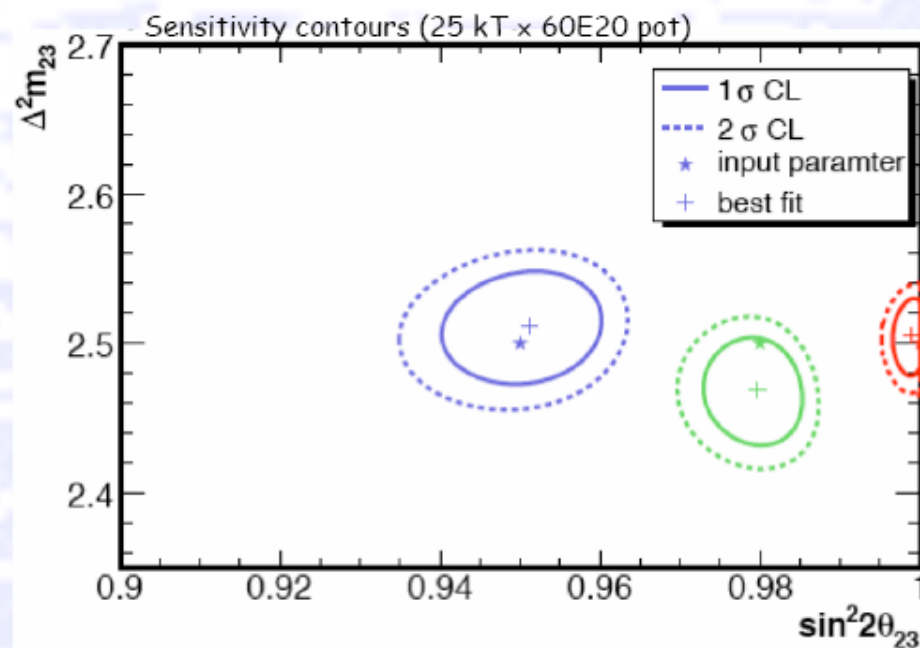
Precise Determination of $\sin^2(2\theta_{23})$



Narrow-band beam and excellent energy resolution allow a high-precision test of a possible new symmetry ($\sin^2 2\theta_{23} = 1$) by measuring QE ν_μ CC events

If $\sin^2(2\theta_{23}) = 1$ it can be measured to 0.004.

Otherwise, it can be measured to ~ 0.01 .



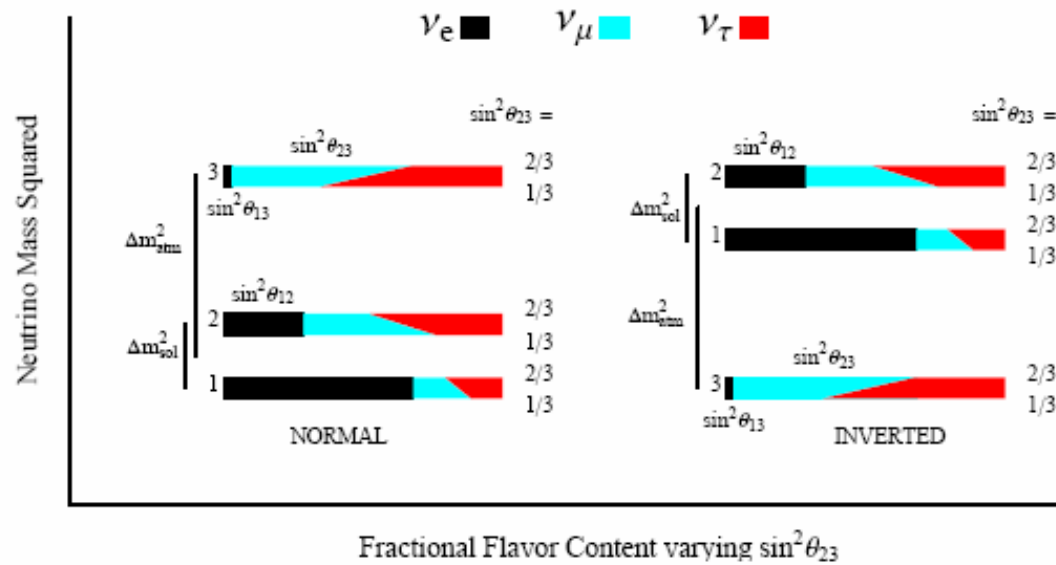
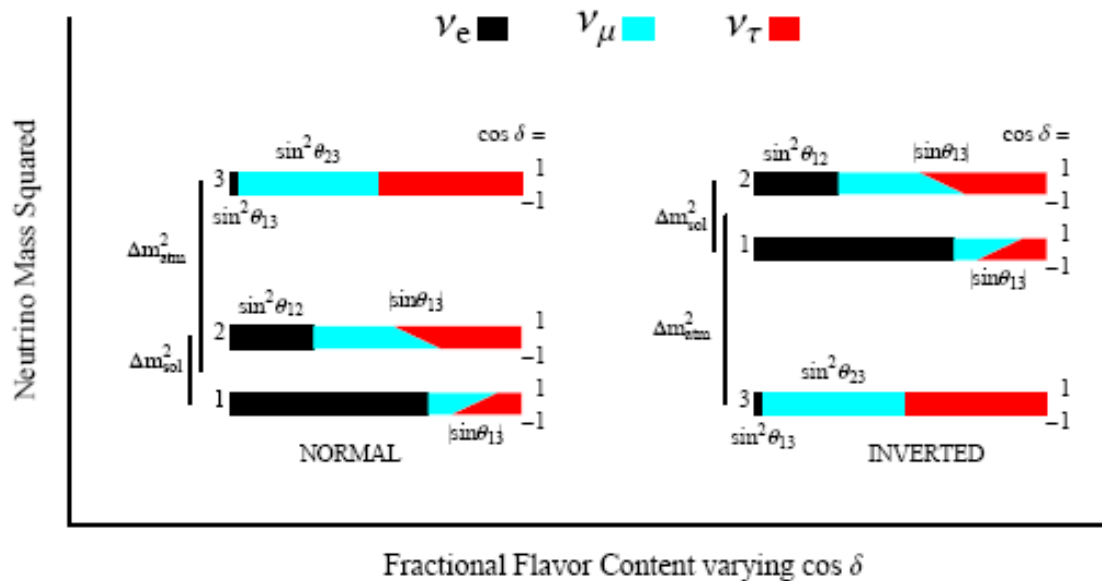


FIG. 1: The range of probability of finding the α -flavor in the i -th mass eigenstate as indicated for the two different mass hierarchies as $\sin^2 \theta_{23}$ varies over its allowed range at the 90% C.L. The bottom of the bars is for the minimum allowed value of $\sin^2 \theta_{23} \approx 1/3$ and the top of the bars is for the maximum value of $\sin^2 \theta_{23} \approx 2/3$. The other mixing parameters are held fixed: $\sin^2 \theta_{12} = 0.30$, $\sin^2 \theta_{13} = 0.03$ and $\delta = \frac{\pi}{2}$.



Unified Graphical Summary
of Neutrino Mixing Parameters

Steven Parke & Olga Mena
hep-ph/0312131

How astrophysical neutrino sources could be used for early measurements of neutrino mass hierarchy and leptonic CP phase

- 1 Considers neutrino fluxes from neutron sources, muon sources and damped pion sources as a ratio of muon flux to e plus tau flux, which can be extracted from neutrino telescopes. Assumes no new phenomena such as neutrino decay.
No distinction is made between neutrinos and antineutrinos.
Muons are identified by Cerenkov light, ν_e by EM showers.
 τ s and ν_e are difficult to distinguish.
Neutral current interactions are a background subtraction.
Statistics on an astronomical ν source may be $\sqrt{10}$ below that of reactor and superbeams.
- 2 The ratio does not measure oscillation parameters in itself, but is very complementary to the reactor and beam measurements, and can improve the sensitivity when all measurements are combined.
- 3 If θ_{13} is large, a measurement of R can not only lead to an early measurement of the CP phase, but can solve the mass hierarchy as well.
- 4 It may even be possible to obtain a measurement of the CP phase with a result from Double CHOOZ alone, with no input from superbeams.
- 5 If θ_{13} is small, a measurement of R can help to remove the octant degeneracy better than a reactor experiments and superbeams alone.
- 6 An additional observation – the electromagnetic to hadronic shower ratio – at a neutrino telescope could be beneficial for pion sources.

$$R = \phi_{\mu} / (\phi_e + \phi_{\tau}) = \phi_{\mu} / (Total - \phi_{\mu})$$

Neutron Beam Source	Pion beam Source	Muon damped Source
Neutron decays	Pion decays	Pi decay with absorbed muon
(e:mu:tau)		
(1:0:0)	(1:2:0)	(0:1:0)
R~0.26	R~0.5	R~0.66

R may also have an energy dependence characteristic of the source.

The mass eigenstates lose coherence because of long distances

Assuming the source is many wavelengths from the earth, the oscillations average to the central value. Small variations are a measure of θ_{13} and δ_{CP}

$$P_{\alpha\beta} = \sum_{i=1}^3 |U_{\alpha i}|^2 |U_{\beta i}|^2$$

Difference in sign

interchange;

role of
0 and π .

$$= \delta_{\alpha\beta} - 2 \sum_{i < j} \text{Re}(U_{\alpha i} U_{\alpha j}^* U_{\beta i}^* U_{\beta j})$$

$$R^{\text{Neutron beam}} \sim 0.26 + 0.30\theta_{13} \cos \delta_{CP}$$

$$R^{\text{Muon damped}} \sim 0.66 - 0.52\theta_{13} \cos \delta_{CP}$$

$$R^{\text{Pion beam}} \sim 0.50 - 0.14\theta_{13} \cos \delta_{CP}$$

Astrophysical telescopes do not distinguish
between neutrino or anti-neutrino.

For superbeams at the first maximum:
Select on neutrino or anti-neutrino.

CP

Even Odd

$$P_{\mu e} \sim 2\theta_{13}^2 \pm 0.09\theta_{13} \sin \delta_{CP}$$

δ_{CP} is suppressed

Strong dependence on θ_{13}

Small perturbation
Amplitude of signal

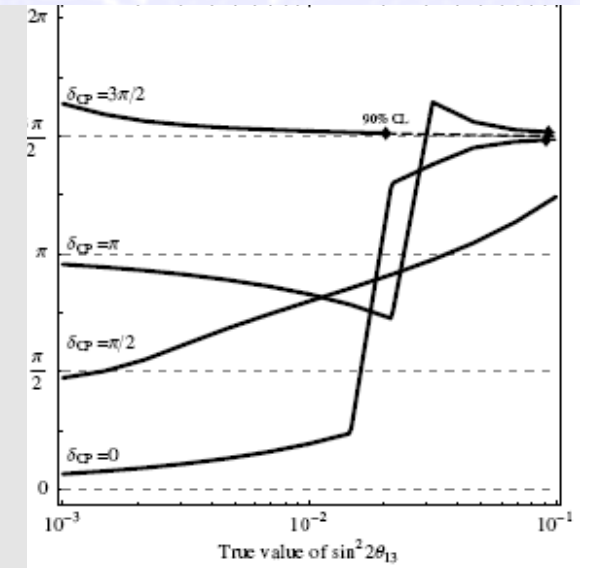
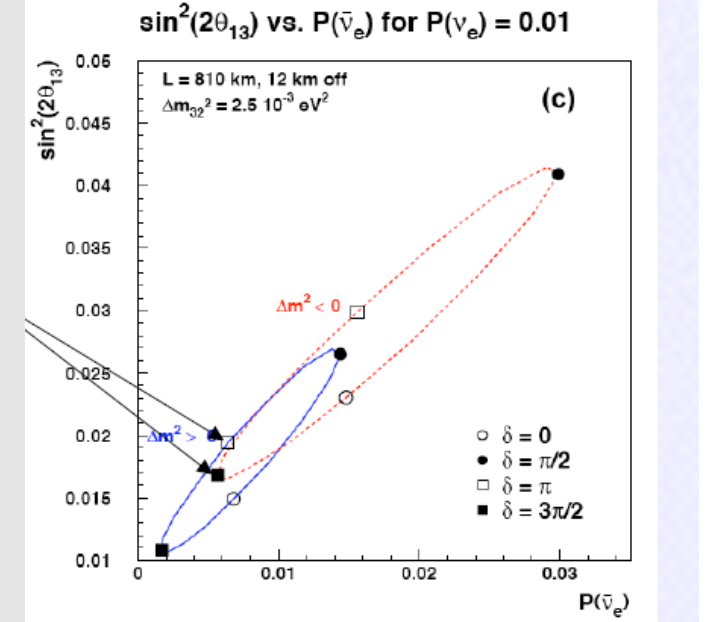
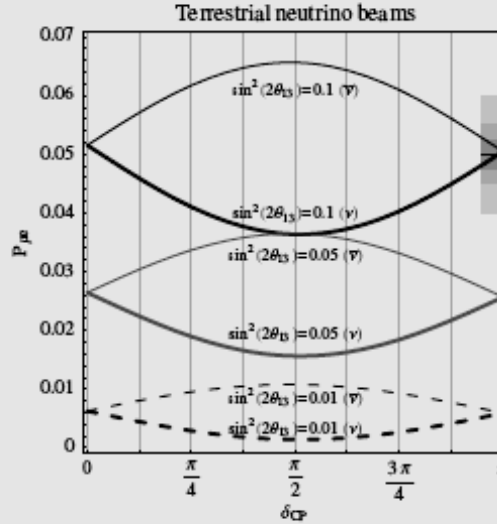
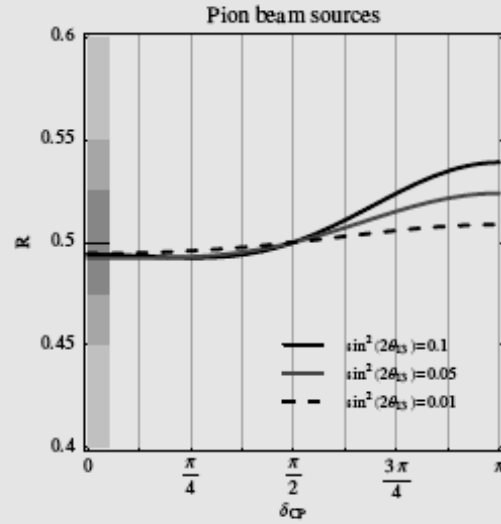
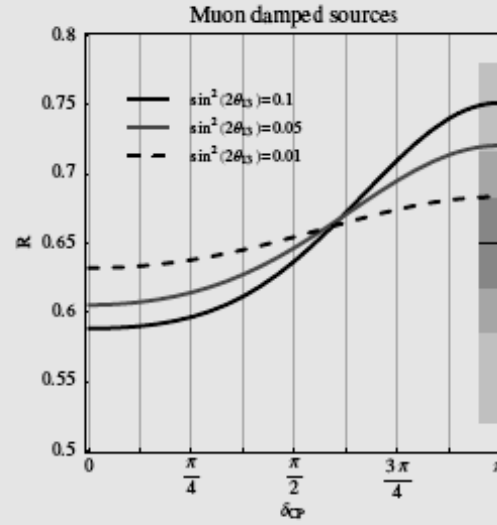
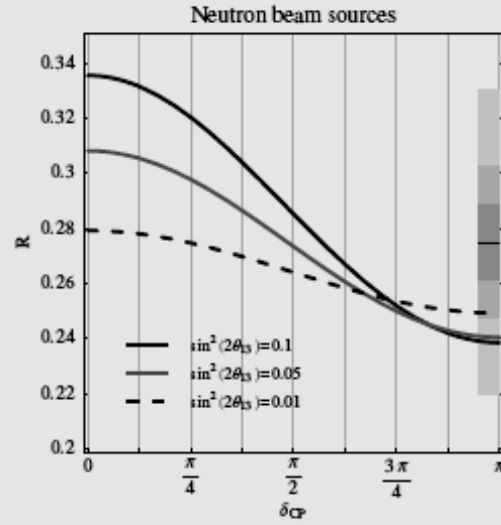
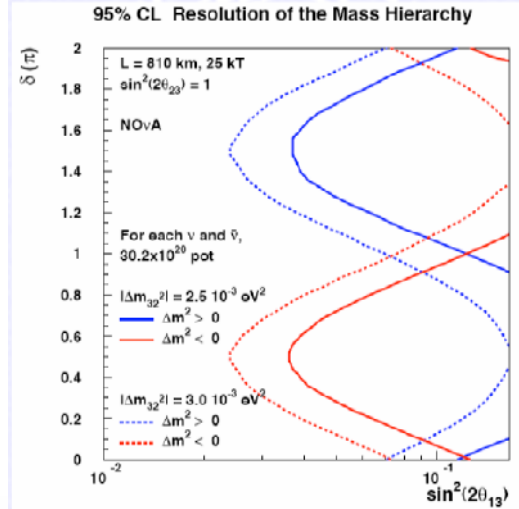


Figure 1: Sources used in this study for which the signal depends on δ_{CP} . We show the quantities R and $P_{\mu e}$ ($P_{\bar{\mu} e}$), respectively, as function of δ_{CP} for different values of $\sin^2 2\theta_{13}$. The shaded bars illustrate the size of the 5%, 10%, and 20% errors for the chosen central values (horizontal lines). For the terrestrial neutrino beam, we assume vacuum oscillations (or short enough baselines) and a measurement at the atmospheric oscillation maximum.

Neutron Beam Source	Pion beam Source	Muon damped Sourde
Neutron decays	Pion decays	Pi decay with absorbed muon
(e:mu:tau)		
(1:0:0)	(1:2:0)	(0:1:0)
R~0.26	R~0.5	R~0.66

	S	C		0.82948	0.535075	0.160182		
12	0.542074	0.84033						
23	0.707107	0.707107		-0.47849	0.532805	0.697976		
13	0.160182	0.987087		0.288124	-0.6556	0.697976		
$\sin^2 2\theta_{23} = 1$								
$\sin^2 2\theta_{12} = 0.83$		e		0.688037	0.286305	0.025658	1	1
$\sin^2 2\theta_{13} = 0.1$		mu		0.228948	0.283881	0.487171	2	1
$\Delta m_{31}^2 = 2.5 \times 10^{-3} \text{ eV}^2$		tau		0.083015	0.429814	0.487171	3	1
$\Delta m_{21}^2 = 8.2 \times 10^{-5} \text{ eV}^2$								
$\delta_{CP} = 0$				1	1	1		
	1			1	1			
Pee	0.473394			0.081971	0.000658	0.556023		
Pemu	0.157525			0.081277	0.0125	0.251301		
Pet	0.057118			0.123058	0.0125	0.192675	1	
Pmue	0.157525			0.081277	0.0125	0.251301		
Pmumu	0.052417			0.080588	0.237335	0.370341		
Pmut	0.019006			0.122016	0.237335	0.378358	1	
				RN=		0.335651		
				Rpi=		0.494012		
				Rmu=		0.588161		

Resolving the Mass Hierarchy



Ron Ray
DOE Review

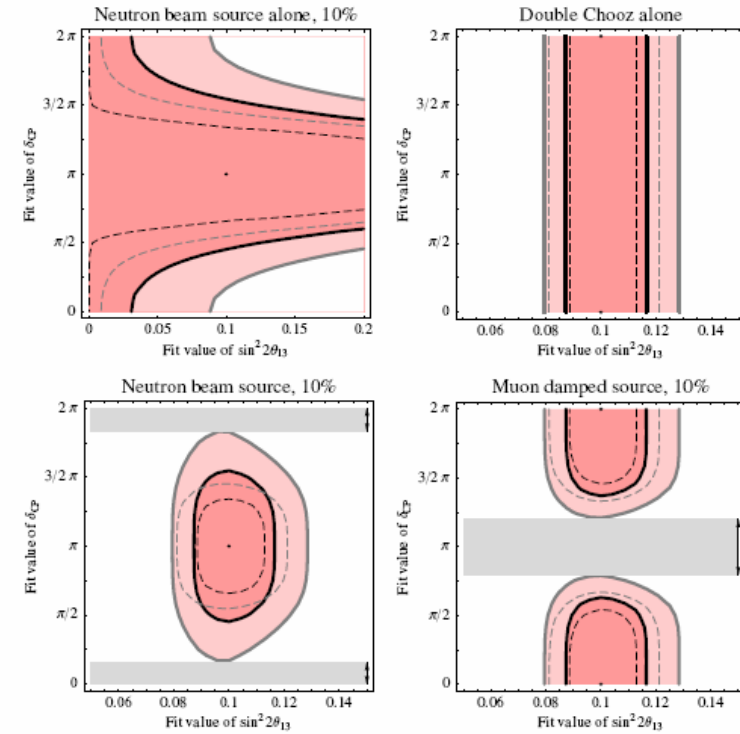
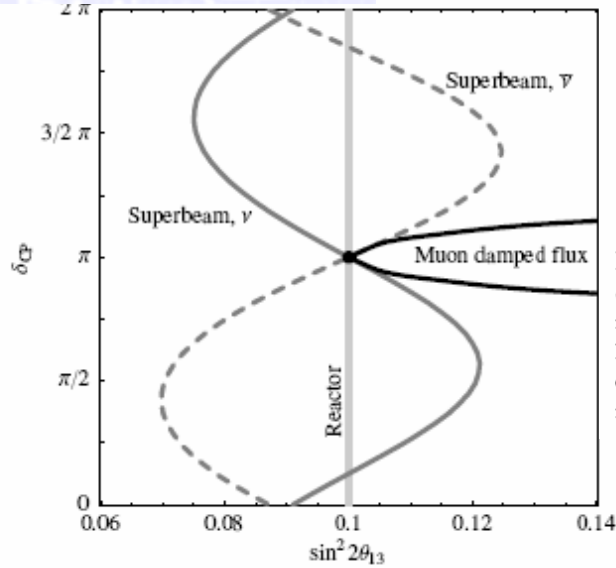


Figure 3: Fit regions as function of $\sin^2 2\theta_{13}$ and δ_{CP} for different experiments as given in the plot captions (the lower row is always in combination with Double Chooz). The simulated values are chosen as marked by the dots. The contours are shown for the 1σ (black curves, dark regions) and 90% (gray curves, light regions) confidence level (1 d.o.f.). Dashed curves represent the results when the other (not shown) oscillation parameters are fixed, *i.e.*, not marginalized over. The arrows in the lower row mark the ranges in δ_{CP} which can be excluded at the 90% confidence level.

Figure 2: Illustration of the synergy among superbeams, reactor experiments, and astrophysical fluxes (at the example of a muon damped source) in $\sin^2 2\theta_{13}$ - δ_{CP} -space. Shown are the curves for constant rates (superbeam, reactor experiment) and constant R (astrophysical flux) going through the best-fit point $\sin^2 2\theta_{13} = 0.1$ and $\delta_{CP} = \pi$.

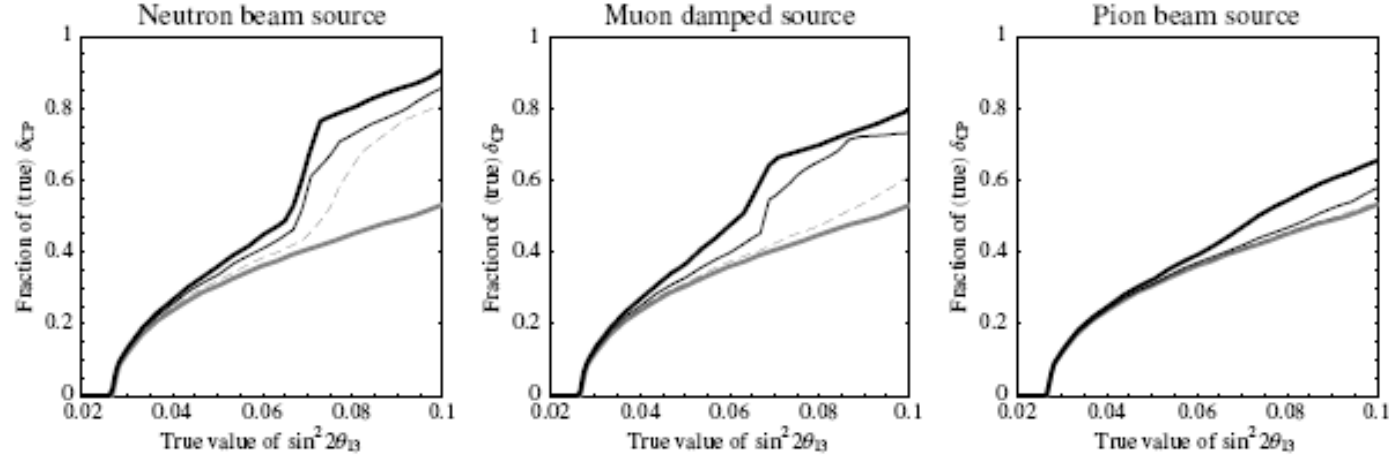
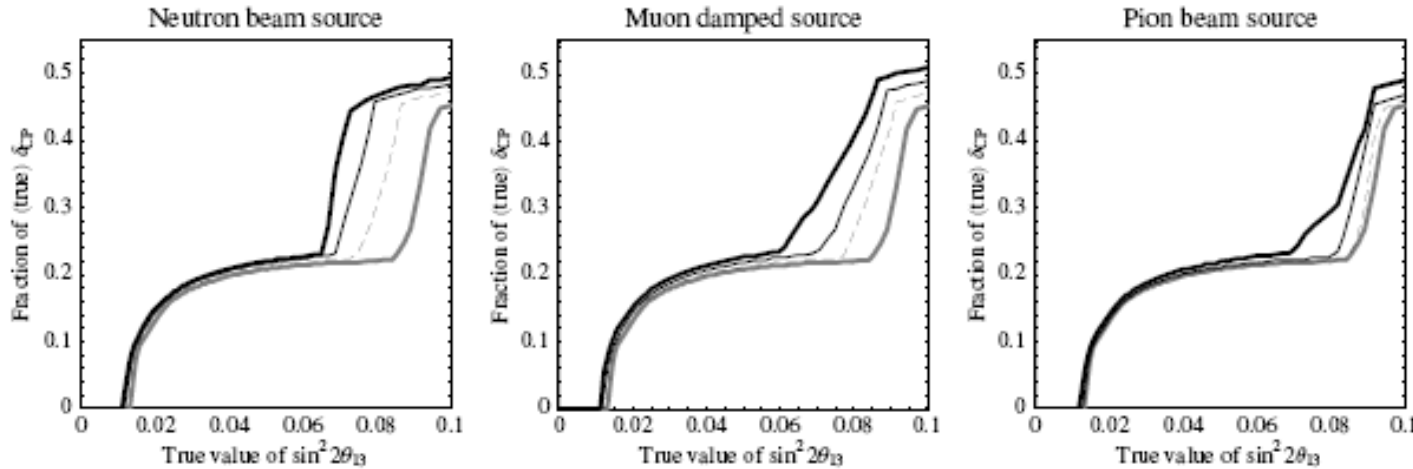


Figure 5: Sensitivity to the normal mass hierarchy as function of true $\sin^2 2\theta_{13}$ and true δ_{CP} (stacked to the “Fraction of δ_{CP} ”) for MINOS, Double Chooz, T2K, and NO ν A combined with an astrophysical neutrino source (as given in the plot captions) at the 2σ confidence level. The curves are for the following errors on the astrophysical flux ratio: no astrophysical flux observed (thick gray curves), 20% error on R (dashed curves), 10% error on R (thin black curves), and 5% error on R (thick black curves).



MINOS, T2K and Double Chooz combined do not have the sensitivity to resolve the mass hierarchy. Nor does NoVA. All of these in combination with astrophysical results will be able to untangle the mass heirarchy, CP phase and θ_{13} .

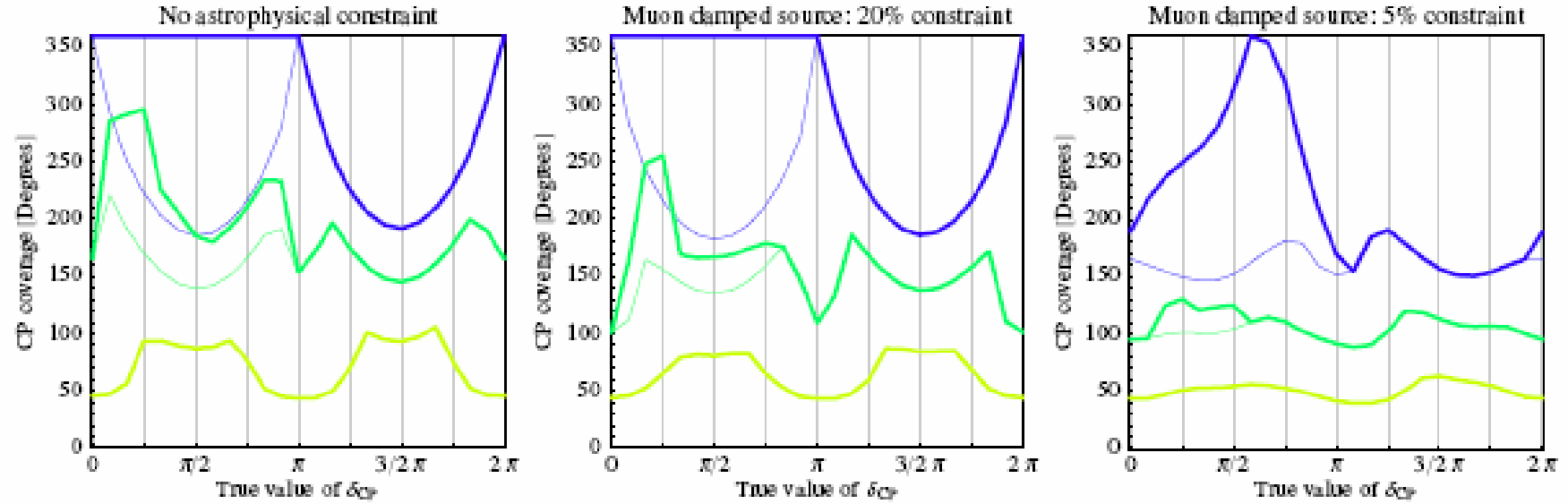


Figure 8: CP patterns for MINOS, Double Chooz, T2K, and NO ν A combined for several external precisions on R from an astrophysical muon damped source. The CP patterns quantify the measurement of δ_{CP} (CP coverage) as a function of the true value of δ_{CP} (provided by nature) for $\sin^2 2\theta_{13} = 0.1$. The CP coverage is defined as range of fit values of δ_{CP} which fit the chosen true value, and can be between 0 (precise determination of δ_{CP}) and 360° (no information on δ_{CP}). The thick curves correspond (from dark to light) to $\Delta\chi^2 = 9, 4$, and 1 respectively, and the thin curves represent the results without taking into account the $\text{sgn}(\Delta m_{31}^2)$ -degeneracy.

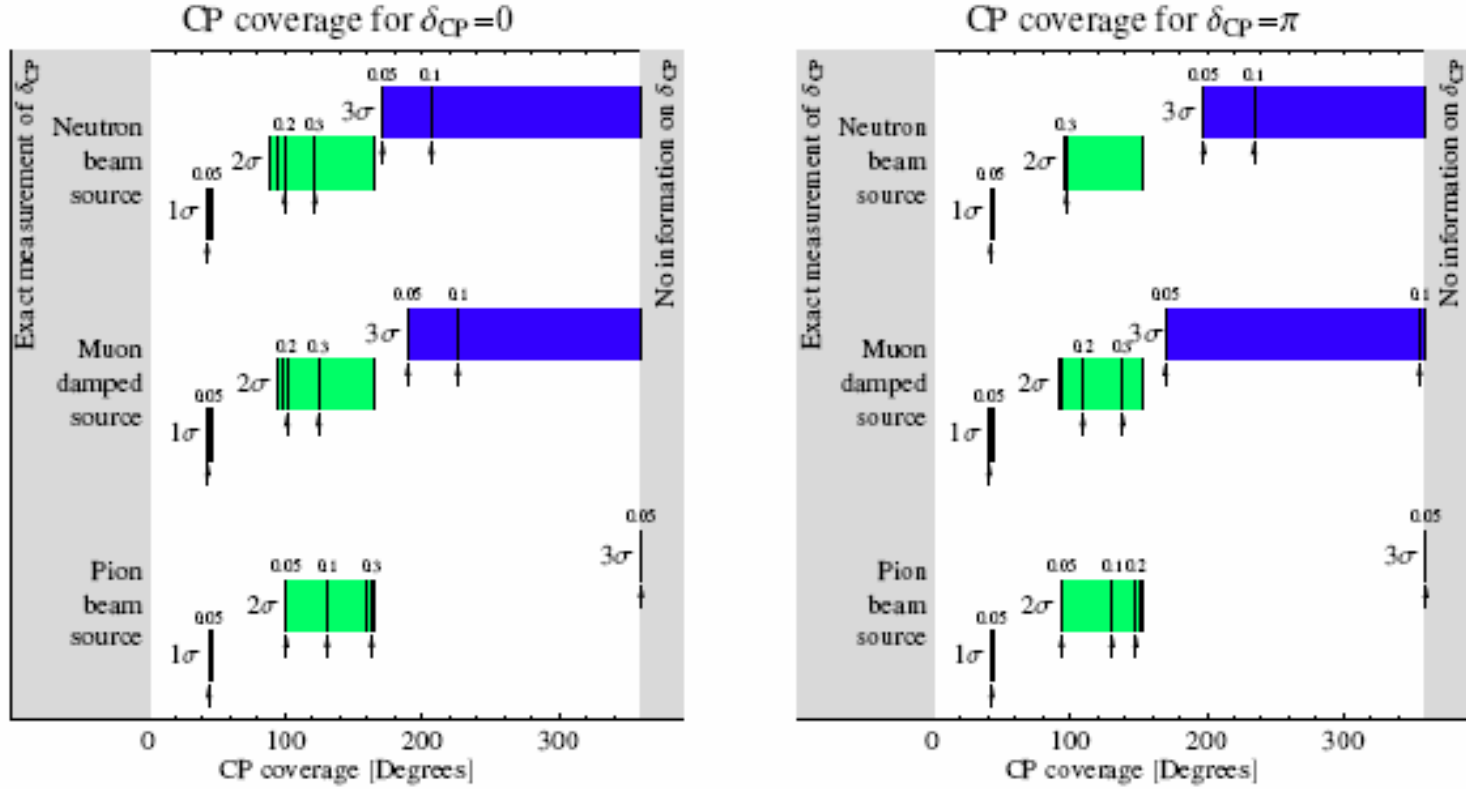


Figure 9: Impact of an astrophysical flux ratio measurement on the CP coverage for MINOS, Double Chooz, T2K, and NO ν A combined for the true $\delta_{CP} = 0$ (left) and π (right), as well as $\sin^2 2\theta_{13} = 0.1$. The bars represent the 1σ , 2σ , and 3σ measurements ($\Delta\chi^2 = 1, 4, 9$) for different astrophysical sources as given in the plots. The right edges of the bars correspond to no astrophysical information, whereas the left edges correspond to a 5% measurement if the respective flux ratio. The vertical lines in the bars represent (from right to left) no astrophysical information, a 30% precision, a 20% precision, a 10% precision, and a 5% precision, where only some of the lines are labeled.

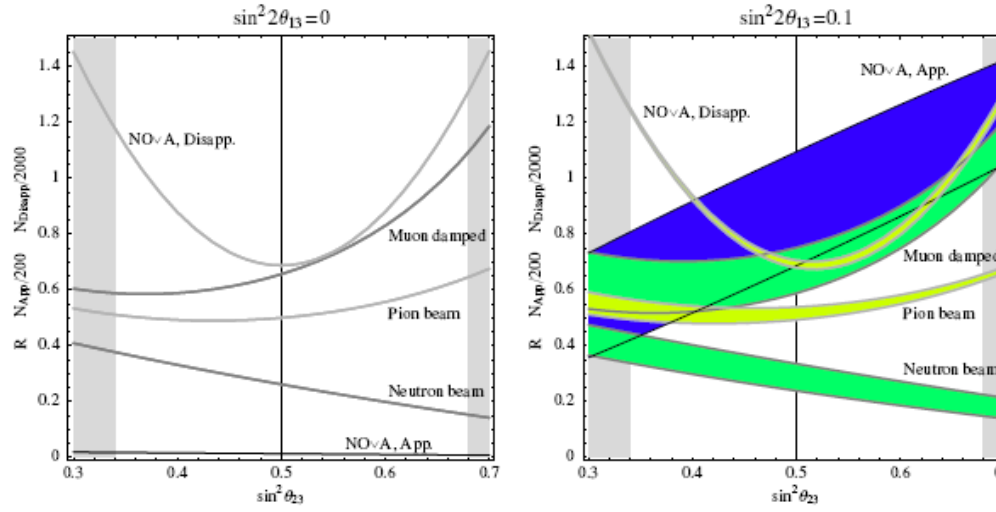


Figure 10: Illustration of the observables (R for astrophysical sources, total event rates for the beam) for the octant degeneracy resolution as function of $\sin^2 \theta_{23}$ for $\sin^2 2\theta_{13} = 0$ (left) and $\sin^2 2\theta_{13} = 0.1$ (right). The bands reflect the unknown value of δ_{CP} . Note the scaling of the vertical axes depending on the source considered. The gray-shaded areas mark the 3σ excluded region [45]. For $NO\nu A$, we assume five years of neutrino running for this figure.

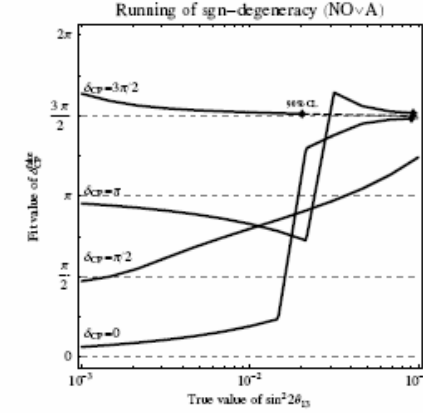


Figure 4: False solution δ_{CP} for the $\text{sgn}(\Delta m_{31}^2)$ -degeneracy as function of the true $\sin^2 2\theta_{13}$ for different values of the true δ_{CP} as given in the plot. Diamonds mark the points beyond which (to the right) the degeneracy can be resolved at the 90% confidence level. Figure for $NO\nu A$ (3 yr neutrinos+3 yr antineutrinos) and a normal hierarchy.

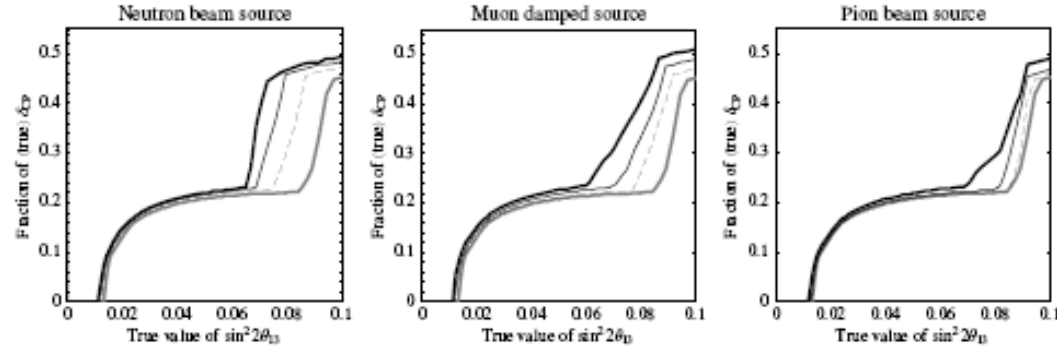


Figure 6: Sensitivity to CP violation as function of true $\sin^2 2\theta_{13}$ and true δ_{CP} (stacked to the “Fraction of δ_{CP} ”) for MINOS, Double Chooz, T2K, and $NO\nu A$ combined with an astrophysical neutrino source (as given in the plot captions) at the 2σ confidence level (normal mass hierarchy assumed). The curves are for the following errors on the astrophysical flux ratio: no astrophysical flux observed (thick gray curves), 20% error on R (dashed curves), 10% error on R (thin black curves), and 5% error on R (thick black curves).

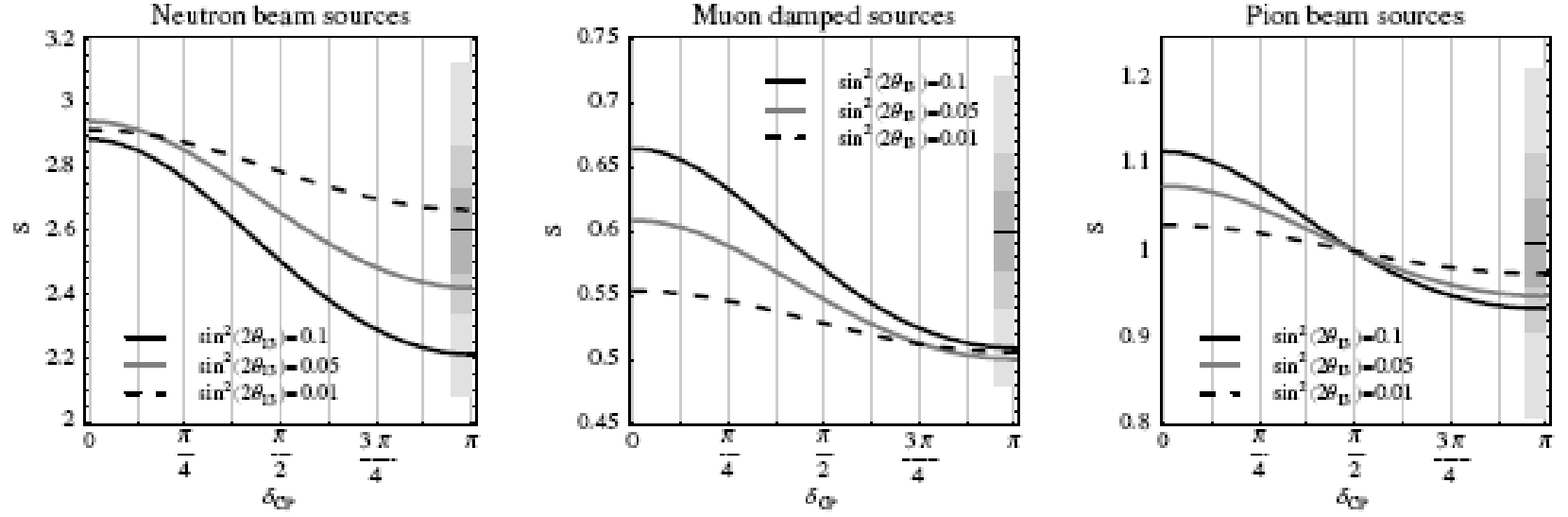


Figure 13: The ratio $S = \phi_e/\phi_\tau$ (representing the electromagnetic versus hadronic shower events) as function of δ_{CP} for the astrophysical sources. The shaded bars illustrate the size of the 5%, 10%, and 20% errors for the chosen central values (horizontal lines).

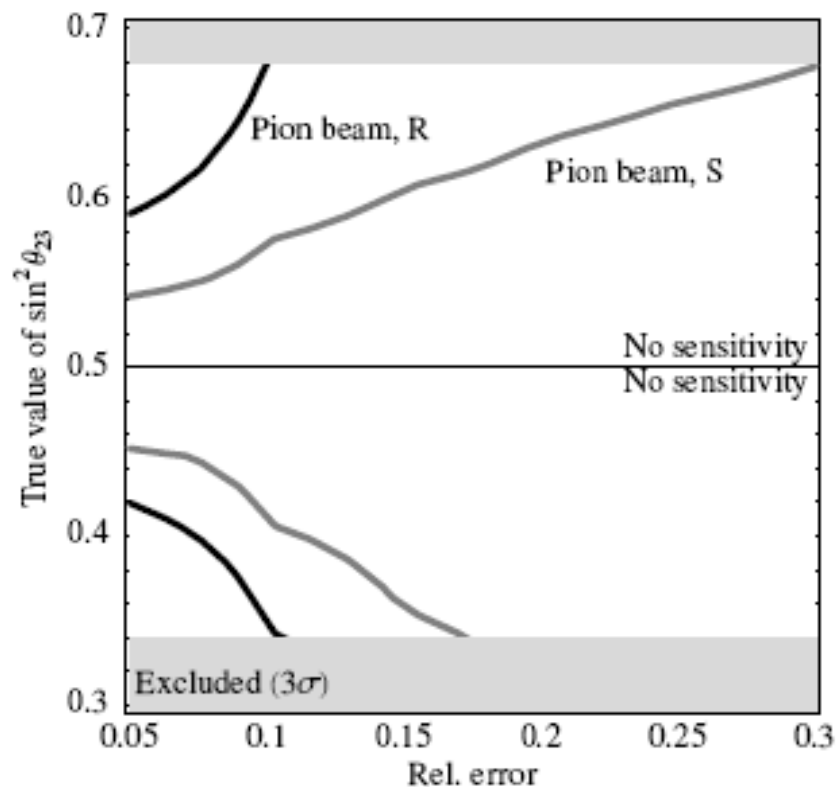
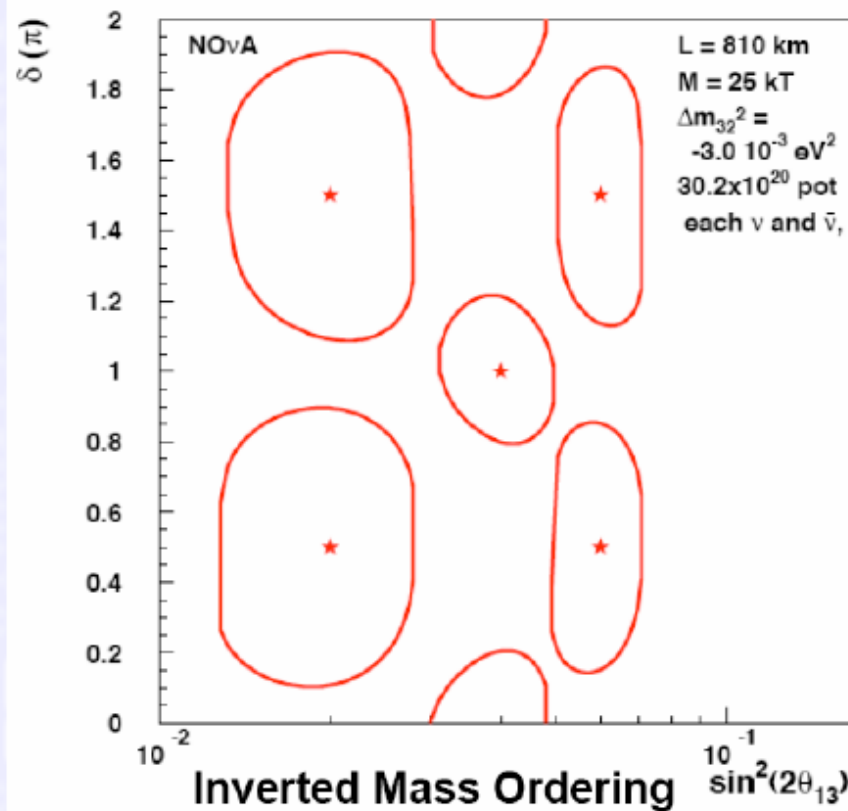


Figure 15: Exclusion of the octant degeneracy as function of either the relative error on R or S , and $\sin^2 \theta_{23}$ at the 2σ confidence level for $\sin^2 2\theta_{13} = 0$. The curves represent the terrestrial experiments (MINOS, Double Chooz, T2K, and NO ν A combined) in combination with an astrophysical pion beam flux. The gray-shaded areas mark the 3σ excluded region [45].

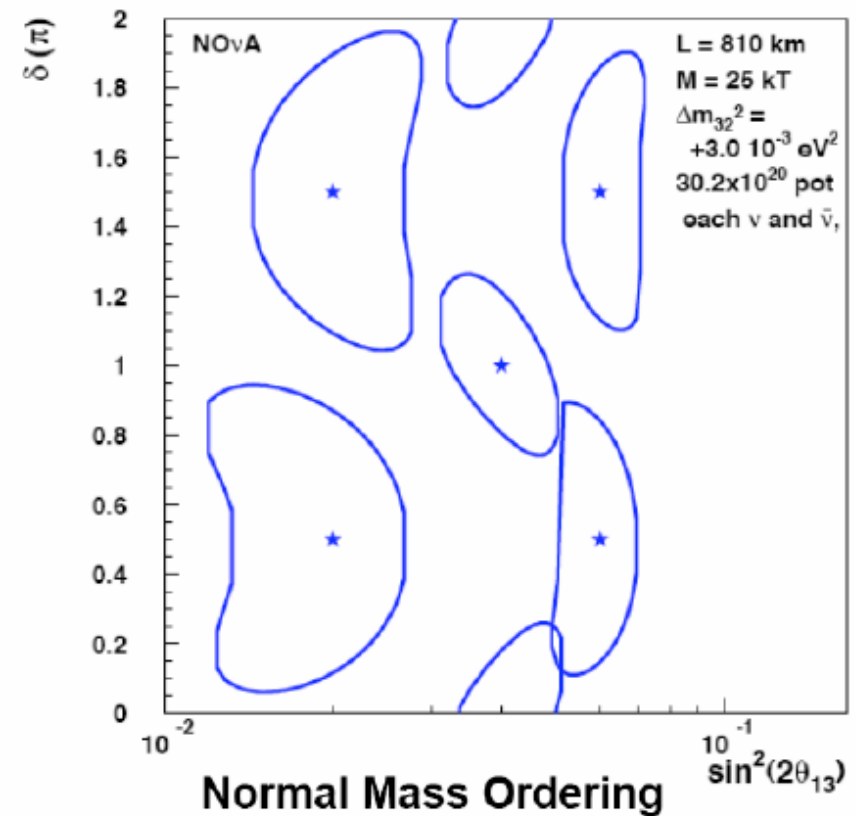


δ vs. $\sin^2(2\theta_{13})$ Contours

1 σ Contours for Starred Points

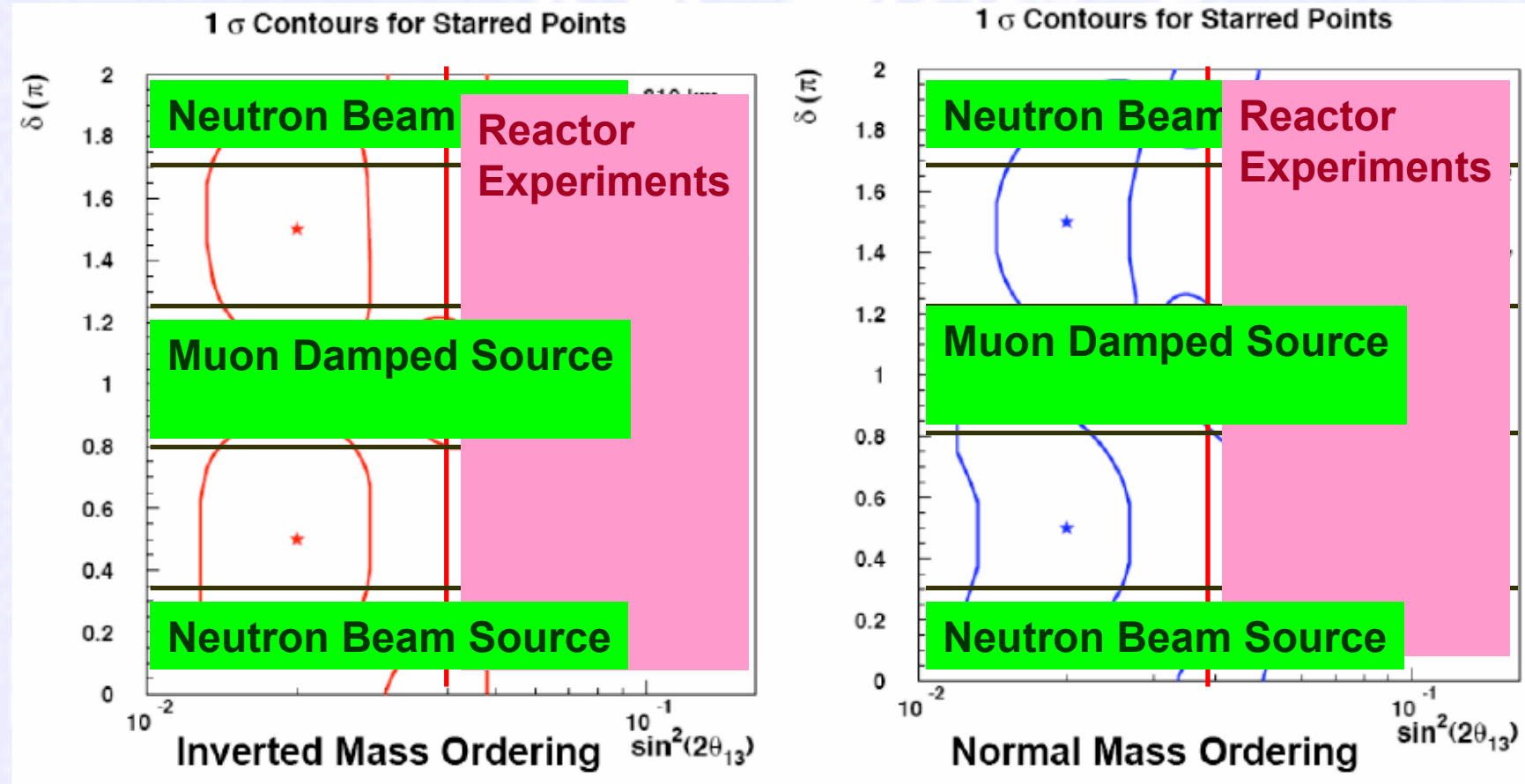


1 σ Contours for Starred Points





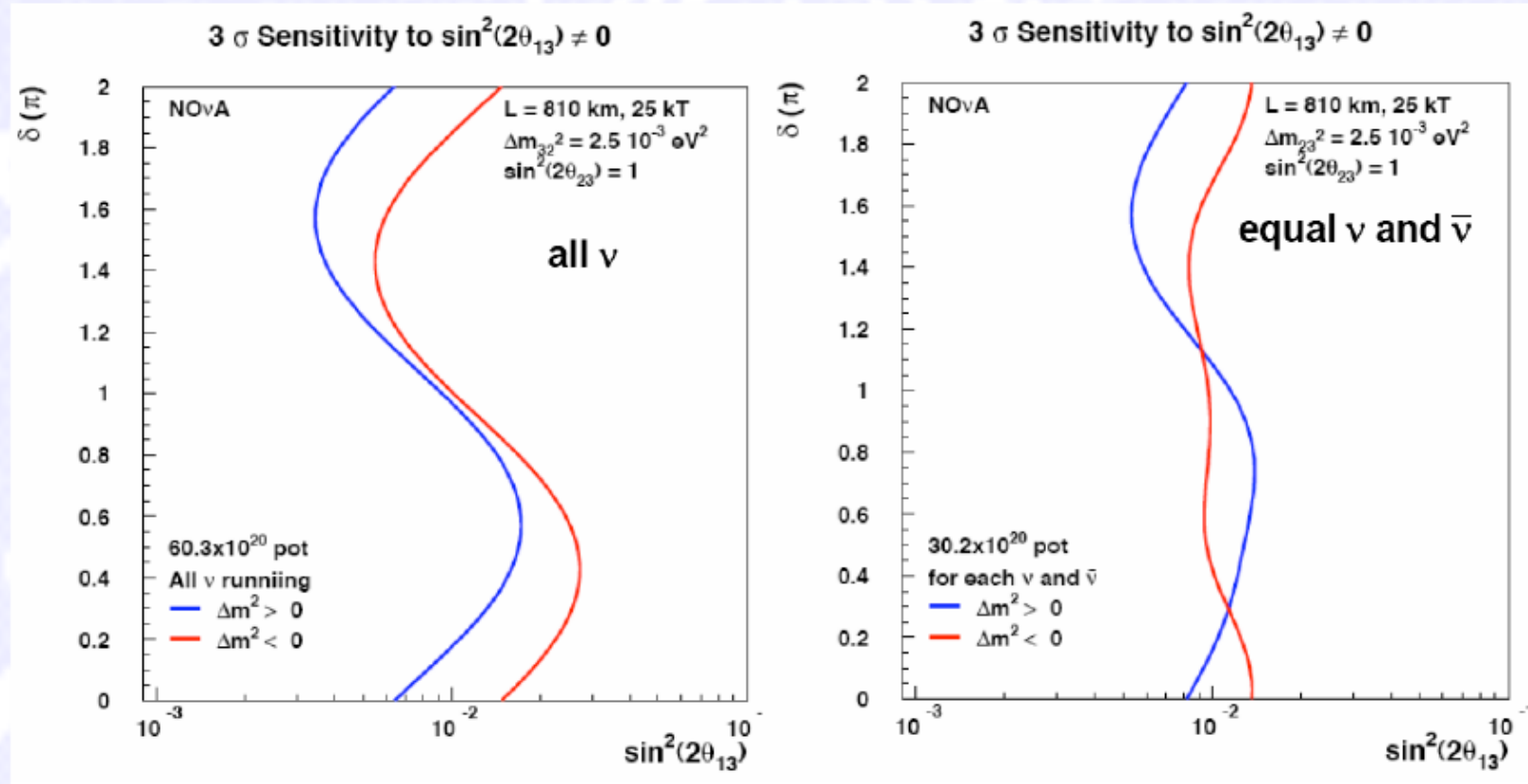
δ vs. $\sin^2(2\theta_{13})$ Contours



Double CHOOZ will set a limit at about 0.02-0.03.



3σ Sensitivity to $\theta_{13} \neq 0$



Values of $\sin^2(2\theta_{13})$ for which NOvA can make a 3σ observation of ν_e appearance. Left plot shows sensitivity for a 6 year neutrino run. Plot on right is for 3 years of neutrinos and 3 years of anti-neutrinos.

